Leveraging Swelling Polymer Nanoparticle Reversibility for Cargo Loading

Beza Tuga^{1, §}, Andrea T. Ligocki^{1, §}, Christy L. Haynes^{1*}

¹ Department of Chemistry, University of Minnesota, Minneapolis, MN, 55455, United States

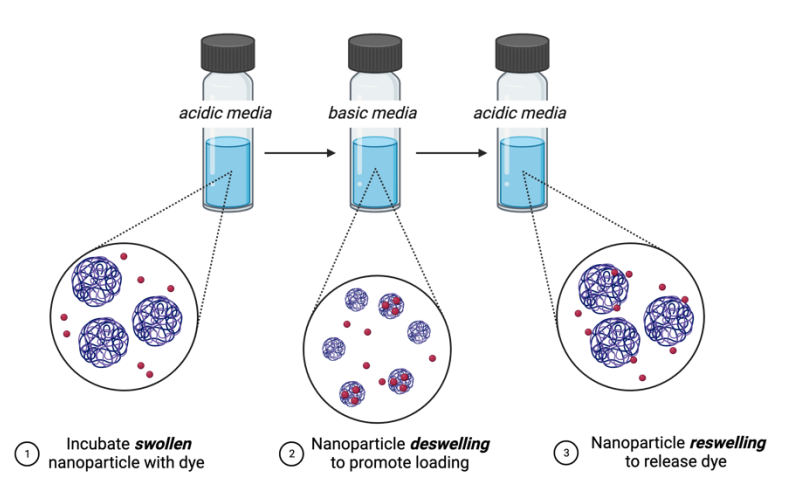
§Denotes equal contributions

*Corresponding author: chaynes@umn.edu

Keywords: Swelling polymer, nanoparticle, reversibility, cargo loading, biomedical and agricultural applications,

ABSTRACT

pH-responsive polymeric nanoparticles are an exciting class of stimuli-responsive materials that can respond to changes in pH and, as a result, have been developed for numerous applications in biomedicine such as the loading and delivery of various cargo. One common transformation is a nanoparticle swelling due to the protonation or deprotonation of specific side chain moieties in the polymer structure. When the pH trigger is removed, the swelling can be reversed, and this process can be continually cycled by adjusting the pH. In this work, we are leveraging this swelling-deswelling-reswelling mechanism to develop a simple, fast and easy loading strategy for a class of crosslinked polymeric nanoparticles, poly-2-(diethylamino) ethyl methacrylate (pDEAEMA), that can reversibly swell below pH 7.3, and a dye, rhodamine B isothiocyanate (RITC), as a proof-of-concept cargo molecule while comparing to poly methyl methacrylate (pMMA) nanoparticles as a non-swelling control. A free radical polymerization was used to generate pDEAEMA nanoparticles at three different sizes by varying synthesis temperature. Their pH-dependent swelling and deswelling was extensively characterized using dynamic light scattering and transmission electron microscopy which revealed a reversible increase in size for pDEAEMA nanoparticles in acidic media, whereas pMMA nanoparticles remain constant. Following dye loading, pDEAEMA nanoparticles show significant fluorescence intensity when compared to pMMA nanoparticles, suggesting that the reversible swelling is key for successful loading. Upon acidic treatment, there is a significant decrease in the fluorescence intensity when compared to the dye-loaded nanoparticles in basic media which could be due to dilution of the dye when released in the acidic media solution. Interestingly, nanoparticle size had no impact on dye loading properties suggesting that the dye molecules only go so far into the polymer nanoparticle. Additionally, confocal microscopy images reveal pDEAEMA nanoparticles with higher RITC fluorescence intensity and contrast in acidic media, but a lower RITC fluorescence intensity and contrast in basic media while pMMA nanoparticle show no differences. Together, these results showcase a size reversibility driven cargo loading mechanism that has potential to be applied to other beneficial cargo and for various applications.



INTRODUCTION

Active nanomaterials hold great promise in a range of application areas, including agriculture, medicine, and sensing, and are often made from stimuli-responsive polymers which are a special class of polymeric materials that can respond to changes in their environmental conditions and are thus often referred to as smart or intelligent materials. ¹⁻³ These polymers can be synthesized to respond to various stimuli such as temperature^{4, 5}, pH^{6, 7}, light⁸, and redox⁹⁻¹¹, among others. For instance, temperature-responsive polymers like poly(N-isopropylacrylamide), pNIPAM, undergo a phase separation at specified critical phase transition temperatures, 4 whereas redox-responsive polymers like polypropylene sulfide (PPS) undergo transitions in solubility or degradation in the presence of reactive oxygen species. 12 With this breadth of stimuli available, progress in this field has led to novel polymeric materials that are responsive to more than one stimulus such as those that contain both a temperature – and pH – responsive group that can undergo differential changes when either temperature or pH is introduced. 13 Given the tunable, smart, and predictable nature of these materials, they have been developed or envisioned for numerous applications in biomedicine such as cargo delivery agents and sensors. ^{1,2} More recently, several stimuli-responsive nanoparticles are being carefully designed and synthesized for applications in sustainable agriculture¹⁴ and due to their active nature, stimuli-responsive polymers have also drawn interest in this field. 15-17

Of the various stimuli available, pH has obvious benefits for biomedical applications due to the natural pH gradient present in cellular environments, especially in cancerous cells.¹⁸ Additionally, plant components like the leaf apoplast have similar pH gradients that allow for pH to be a viable trigger in agricultural applications.^{19, 20} A characteristic feature of pH-responsive

polymers is the presence of ionizable moieties in their structure that can be protonated or deprotonated as the pH changes, driven by the polymer's pKa. Thus, when choosing a pH-responsive polymer for a desired application, it is important to be mindful of the pH range in which a response is desired.²¹ Another important factor to consider is the structural properties of the polymers, which can be synthesized as linear, crosslinked, branched, or networked forms that are often assembled to form polymer-based nanoparticles (or polymeric nanoparticles).^{22, 23} In addition, exposure to pH changes can impact polymer nanoparticle structure, inducing disassembly, swelling, or rearrangement due to the aforementioned ionization.^{7, 21} The work detailed herein will focus on pH-induced changes to polymer nanoparticle swelling, a pH-dependent size transformation of polymers that results in an increase in size. More specifically, this occurs in 3 sequential events following pH exposure: 1) the protonation or deprotonation of polymer pendant groups, 2) charge build up to generate electrostatic repulsion throughout the polymer structure, and 3) size increase (or swelling).

A commonly used pH-responsive polymeric nanoparticle, and one investigated here, is poly-2-(diethylamino)ethyl methacrylate (pDEAEMA). pDEAEMA nanoparticles are easy to synthesize and are prepared from commercially available and inexpensive starting materials making them advantageous over other pH-responsive materials.²⁴ They also undergo pH-based transitions at physiologically and ecologically relevant pH values, giving them potential for a range of application areas.²⁵ In the context of cancer treatment, using nanoplatforms like pDEAEMA, can aid in compensating negative side effects of traditional cancer treatments. ²⁶ pDEAEMA contains tertiary amine groups in its chemical structure (Figure 1), and as such, pDEAEMA is categorized as a basic polymeric nanoparticle because it can be protonated.²¹ When protonated, the nanoparticles increase in size at a pH ≤ 7.3 due to the pKa of the tertiary amine group; for pDEAEMA, this property can also be reversed when the pH is reversed. Due to this pH-dependent transformation and tunable synthesis characteristics, pDEAEMA-based materials are being designed for cargo loading and release applications. Wong et al. synthesized a dual component polymer system prepared from a homopolymer pDEAEMA component and a diblock copolymer poly(2-(diethylamino)ethyl methalcrylate)-b-poly(ethylene glycol) component where the pDEAEMA is driving the pH-dependent disassembly, and release, within the highly acidic endosome of fibroblast cells.²⁷ pDEAEMA was also used by Hern et al. to generate a diblock copolymer to deliver a beneficial peptide that was directly incorporated in the polymer structure

to generate a complex micelle system. The use of a pDEAEMA block allowed for tumor-specific micelle disassembly, facilitating peptide release in a timely and site-specific manner due to the low pH of tumor cells.²⁸ As a result of the predictable pH-based properties, pDEAEMA has also been used in conjunction with other non-polymeric materials like silica nanoparticles. Sun et al. used surface-initiated atom transfer radical polymerization to prepare core-shell nanoparticle system with a mesoporous silica nanoparticle (MSN) core and pDEAEMA shell.²⁹ pDEAEMA served as a pH-controlled switch to regulate the opening and closing of the pores present on the MSN surface, thereby allowing for rapid release in acidic media, but slow release in basic media. The open/closed state of these pores was reversible which showcases an important, yet underutilized, characteristic of pH-responsive swelling polymers – their reversibility. When the swollen pDEAEMA nanoparticle is placed in a pH \geq 7.3, pDEAEMA reverts to its original size, and, if desired, the size can be increased and decreased repeatedly. Herein, we aim to use this property of pDEAEMA nanoparticles as a novel cargo-loading method. As evidenced by the studies outlined above, the use of pDEAEMA nanoparticles is a common practice, especially in the context of cargo loading and release. However, the cargo loading process can be time-intensive and laborious. 27, 30-³⁶ This is due to the fact that most loading strategies rely on the passive "post-loading" method where the synthesized polymer nanoparticle is incubated or stirred with the cargo of interest for a significant period of time to enhance loading and adsorption of the cargo to the nanoparticle. 37, 38 In this work, we propose a new, simple, and fast method for loading pDEAEMA nanoparticles by leveraging their robust and predictable swelling-deswelling-reswelling behavior. Unlike the aforementioned papers, the work proposed here shows that cargo loading can be achieved by simply mixing the cargo with the pDEAEMA nanoparticles while controlling the solution pH with no incubation period.

The goal of this work is to design pH-responsive polymer nanoparticles that can load small molecule cargo, with potential applications in both medicine and agriculture. Taking advantage of the pDEAEMA properties, we incubated our cargo of interest, rhodamine B isothiocyanate (RITC), which is commonly used for fluorescence detection and unresponsive to pH changes, with pDEAEMA in a swollen state and then reversed the swelling to allow for dye uptake as the polymeric nanoparticle shrank. We were also interested in the role of polymer nanoparticle size on dye loading, so we prepared a series of pDEAEMA nanoparticles with sizes ranging from 200 nm – 600 nm in diameter that showed similar nanoparticle swelling and loading behavior. With

tunable overall nanoparticle size and pH-responsive behavior in a biologically relevant pH range that facilitates small molecule loading, these nanoparticles hold great potential across a range of application areas. Additionally, we are confident that this more efficient loading strategy will inspire future work that leverages the reversibility of other stimuli responsive polymeric nanoparticles.

MATERIALS AND METHODS

2-diethylaminoethyl methacrylate (DEAEMA), ammonium persulfate (APS), methyl methacrylate (MMA), and rhodamine B isothiocyanate (RITC) were purchased from Sigma Aldrich. MWCO 10,000 dialysis tubing and dimethyl sulfoxide (DMSO) were purchased from Thermo Fisher Scientific. Poly(ethylene glycol) dimethacrylate 200 (PEGDMA) was purchased from Polysciences Inc. Unless otherwise noted, chemicals were used as received.

pDEAEMA and pMMA nanoparticles were synthesized by a free radical polymerization as previously reported. ²⁵ In a 50 mL round bottom flask, MilliQ water (9 mL), 2-diethylaminoethyl methacrylate (DEAEMA) (1 mL, 4.87mmol) or methyl methacrylate (MMA) (528 μL, 4.96 mmol), and poly(ethylene glycol) dimethacrylate (PEGDMA) 200 (10 μL, 0.0326 mmol) were mixed by stirring (500 rpm) for 15-30 minutes in an oil bath at 40 °C, 50 °C, or 70 °C. A 50 μL aliquot of 200 mg/mL of the radical initiator ammonium persulfate (APS) was added to the reaction mixture, turning the solution white and opaque. With nitrogen purging directly into solution, the reaction continued for 3 hours. The pDEAEMA nanoparticle suspension was dialyzed in a MWCO 10,000 kDa Fisher Scientific dialysis tube against DI water with gentle stirring for 3 days (with daily water replacement). The particles were purified via ultracentrifugation (Beckman-Coulter Optima L-100K) at 427,635 xg for 20 minutes, redispersed in MilliQ water, and then another 3 rounds in PBS. After 4 total rounds of centrifugation, the pDEAEMA nanoparticles were diluted to a concentration of 19.66 mg/mL with PBS and stored in the refrigerator at 4 °C until further use.

Polymer Nanoparticle Characterization

An aliquot of each size of the pDEAEMA and pMMA nanoparticle suspension (40 μ L) was placed in phosphate buffers (1 mL) ranging from pH 4 to pH 11. Hydrodynamic diameters and zeta potentials were measured using a Malvern Panalytical Zetasizer instrument. The reported hydrodynamic diameter and zeta potential values are the average of three technical measurements across 3 material replicates. To measure the time-based swelling behavior of the nanoparticle, an aliquot (40 μ L) of the nanoparticle was placed in a buffer of pH 4.7 (1 mL), and the hydrodynamic

diameter was measured every 10 minutes for an hour. To test the reversible swelling mechanism, the particle suspension (40 μ L) was placed in pH 4.7 buffer (1 mL), then the hydrodynamic diameter and zeta potential was measured; this solution (500 μ L) was then placed in NH₄OH (500 μ L) at pH 11 and measured again. Finally, the same solution (500 μ L) was placed back into pH 4.7 solution (500 μ L) with the size measured one final time.

Transmission Electron Microscopy

Three different solutions of pDEAEMA and pMMA nanoparticle solutions were prepared with 40 µL aliquots of each nanoparticle solution added to i) water, ii) water spiked with hydrochloric acid, and iii) water spiked with ammonium hydroxide solution. Afterward, 200 mesh copper grids with Formvar and carbon supports (Ted Pella, Inc., Redding CA) were dipped in each of the three solutions and left to air-dry overnight. Images were taken using the Thermo Fisher Talos F200x G2 at a 200 keV acceleration voltage on a Thermo Fisher Ceta camera. To determine the size of the pDEAEMA and pMMA nanoparticles, images were analyzed using Fiji using 500 randomly selected nanoparticles in each of the water-based, acidic, and basic solutions.

Dye Loading and Release

Rhodamine B isothiocyanate RITC (1 mg/mL in DMSO), or water for a non-fluorescent control, was loaded into the pDEAEMA using the nanoparticle's reversible swelling mechanism. An aliquot of 19.66 mg/mL pDEAEMA (240 μ L) was placed into a potassium phosphate buffer solution (1 mL) of pH 4.7 to induce nanoparticle swelling. This solution was incubated on a shaker for 1 hour (150 rpm) to promote polymer-dye association. Half (500 μ L) of this solution was placed in NH₄OH (500 μ L) at pH 10.15 to shrink the pDEAEMA back down and promote dye-loading. This solution was centrifuged (Fischer Scientific accuSpin Micro 17) at 17,000 xg 5 times for 20 minutes, each with a PBS wash to dispose of any dye that was not loaded or associated. The supernatants were collected for fluorescence measurements, placing 200 μ L aliquots in 3 wells on a microplate respectively, as well as their water control counterparts. Half (500 μ L) of the final solution was placed in pH 4.742 buffer (500 μ L) to swell the particle again and release the RITC, while the other half (500 μ L) remained in "basic" PBS with PBS topping it off (500 μ L). Each solution had 200 μ L aliquots placed in 3 microplate wells for measuring, with water controls as well. All of this was also done in parallel with pMMA nanoparticles as a control comparison.

A BioTek Synergy H1 Microplate Reader was used to measure the fluorescence of the final solutions. The excitation wavelength was 556 nm, and the emission wavelength 587 nm based on a fluorescence scan of the RITC/DMSO solution. This fluorescence data was analyzed by averaging 3 well measurements (technical replicates) for each solution, then the average water control values were subtracted from the average dye-loaded values to account for any polymer interference. Three material replicates of each size polymer were loaded and measured in the same way, and the average of these replicates represents the amount of dye taken up by the polymer.

Confocal Microscopy

Slides for confocal microscopy were prepared by placing 5 µL of the loaded sample prepared for the plate reader measurements in the center of a glass slide, placing a number 1.5 cover slip on top without creating air bubbles, and sealed to avoid any evaporation. Using an Olympus Fluorview IX2 Confocal Microscope, images of the loaded nanoparticles on the slide and water controls were taken at 60x magnification. The resulting images were analyzed using Fiji by choosing 300 fluorescent features throughout the image for the pDEAEMA using the default fluorescence threshold and 15 fluorescent features for the pMMA using the triangle threshold (the smaller number and thresholding were necessary due to the lack of fluorescence visible). Each fluorescent feature's area and mean fluorescence intensity were measured in Fiji. The Quick Figures plugin in Fiji was used to prepare confocal images along with insets representing regions of interest.

Statistical Analysis

All statistical analysis testing was conducted using Graph Pad Prism 8 Version 8.4.3. An unpaired t-test was used to compare average TEM diameters, mean fluorescence intensities, and areas in confocal images of pMMA and pDEAEMA nanoparticles, with a p<0.05 indicating statistical significance. To compare size changes during the pH cycling process, we used a paired t-test (p<0.05). Statistical analysis of average fluorescence intensity for pDEAEMA nanoparticles (across 3 sizes) and pMMA nanoparticles was conducted using two-way ANOVA with a Tukey's multiple comparisons test (p<0.05). All error bars represent standard deviation across 3 material replicates.

RESULTS AND DISCUSSION

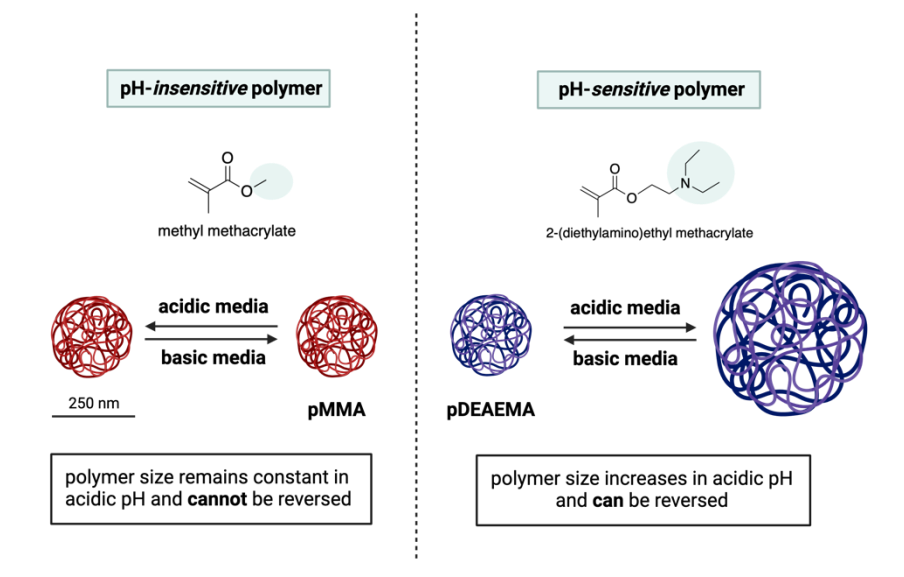


Figure 1: Schematic of polymeric nanoparticles and their properties in different pH media. Figure created with BioRender.com.

Polymer Nanoparticle Characterization

Initial pDEAEMA and pMMA nanoparticle characterization used transmission electron microscopy for morphology and size information and dynamic light scattering for diameters and zeta potentials of the nanoparticles in water as shown in Figure 2. The micrographs in Figure 2A for pMMA and Figure 2B for pDEAEMA show monodisperse polymeric nanoparticles with similar morphologies for both nanoparticles; these are comparable to previously reported syntheses.²⁵ Scanning electron microscopy was also used to compare surface morphology of pDEAEMA and pMMA nanoparticles and shows similar spherical morphologies for both nanoparticles (Figure S5 in the Supporting Information). Additionally, they also have similar hydrodynamic diameters (241.8 \pm 37.2 nm for pMMA and 251.6 \pm 13.2 nm for pDEAEMA) as shown in Figure 2C. As expected, the zeta potential of these two nanoparticles is different, where pDEAEMA displays +31.7 mV while pMMA is -21.9 mV. This is due to the difference in functional groups present in the two nanoparticles – pDEAEMA (structure shown in Figure 1) has a tertiary amine that is prone to protonation while pMMA does not. We measured the molecular weight of pDEAEMA nanoparticles using static light scattering on a Malvern zetasizer and estimate the molecular weight to be ~ 8 kDa. Overall, these particles show similar characteristics in pristine media in advance of pH excursions, allowing for effective comparison of their performance.

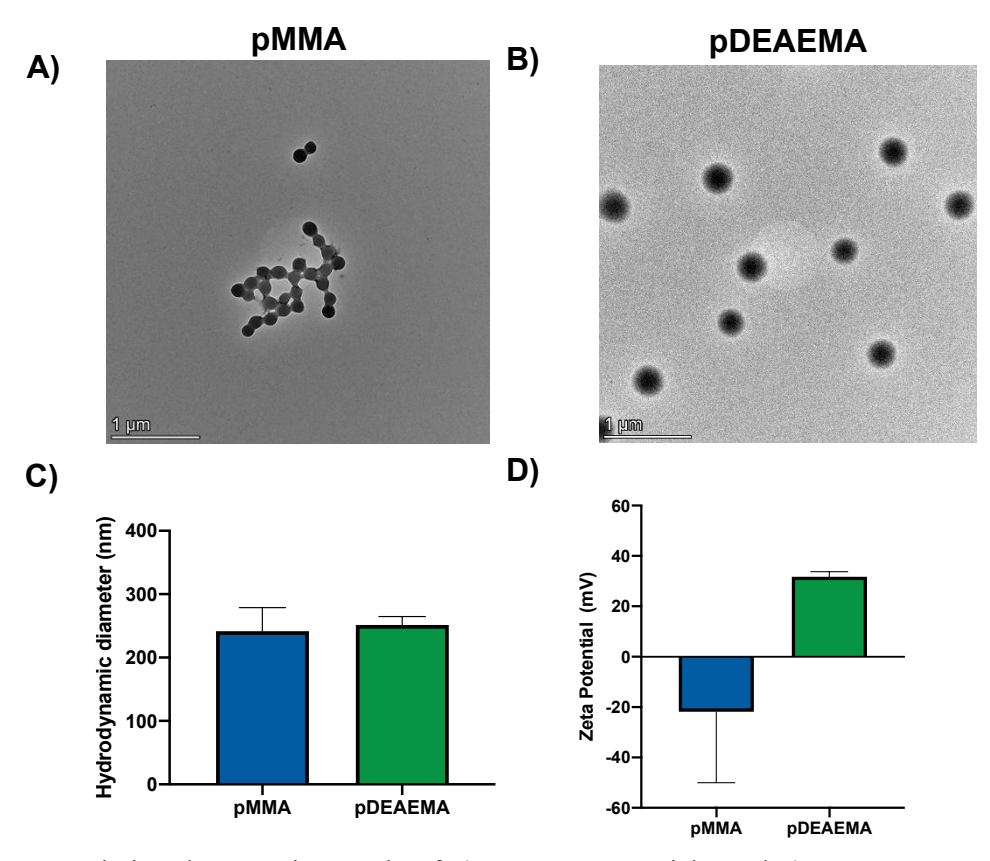


Figure 2: Transmission electron micrographs of A) pMMA nanoparticles and B) pDEAEMA nanoparticles. C) and D) are hydrodynamic diameters and zeta potentials of both nanoparticles, respectively. There is no difference in the hydrodynamic diameters of the two nanoparticles. Error bars represent standard deviations of 3 material replicates for both nanoparticles.

pH-based Polymer Nanoparticle Transformations

Altering the pH microenvironment of pH-responsive polymers results in transformations within the polymer architecture that can lead to swelling or other changes to polymer self-assembly.²¹ In this work, we are interested in leveraging the size-based transformations of pDEAEMA, and as such, we investigated changes in size of this nanoparticle in the presence of different pH media using TEM and DLS as shown in Figure 3 and 4. As these size changes for pDEAEMA are expected to occur at a pH of 7.0 - 7.3, the size measurements in Figure 3 were conducted in two pH conditions: pH > 7.3 (representing basic media) and pH < 7.3 (representing acidic media). The TEM micrographs in Figure 3 show that nanoparticles in media with pH > 7.3 are similar to those shown in Figure 2; however, differences arise when these nanoparticles are placed in media with pH < 7.3 . For pMMA, no change is observed, but for pDEAEMA, reducing

the pH below 7.3 transforms the particles into larger and lower contrast nanoparticles. This is evident in the average TEM diameter in Figure 3B as there is a statistically significant increase in the diameter of the pDEAEMA nanoparticles from 350 ± 23 nm to 523 ± 60 nm when spiked with acid, whereas the diameter of pMMA nanoparticles stays the same (140 ± 15 nm and 160 ± 15 nm when spiked with acid). The turbidity of the pDEAEMA nanoparticle suspension is also affected by the addition of an acid as it transitions from a characteristic cloudy to a clear solution as shown in Figure 3C. This visualization of the phase transition reveals that the increase in pDEAEMA size is instantaneous and can be maintained over time as shown by Figure S1 in the Supporting Information. This pH-based size and turbidity transformation in pDEAEMA occurs due to the protonation of the tertiary amine groups present in pDEAEMA, but not in pMMA. The pKa of these amine groups is between 7.0 - 7.3; thus, when the pH falls below this range, the amine groups are protonated which results in a charge buildup and subsequent polymer nanoparticle size increase (Figure S2 in Supporting Information). To further characterize this property, the pH sensitivity of both pDEAEMA and pMMA nanoparticles was measured using an array of phosphate buffers with pHs ranging from 4 - 10 at room temperature. Figure 4 shows the hydrodynamic diameters and zeta potentials of these nanoparticles as a function of solution pH. For pDEAEMA, the size remains around 200-nm-diameter in basic media and transitions to a size of $\sim 650-700$ nm in diameter at pH 7.3, which is characteristic for pDEAEMA due to the pKa mentioned above. As expected, the size of pMMA is unresponsive to any changes in pH. The zeta potential values also show similar trends for both particles – pDEAEMA nanoparticle zeta potential becomes more positive as the pH drops below 7.3 while pMMA remains largely negative and consistent. All this characterization points to a well-understood pH-driven size transformation in pDEAEMA that has potential utility for loading if the size transformation is reversible.

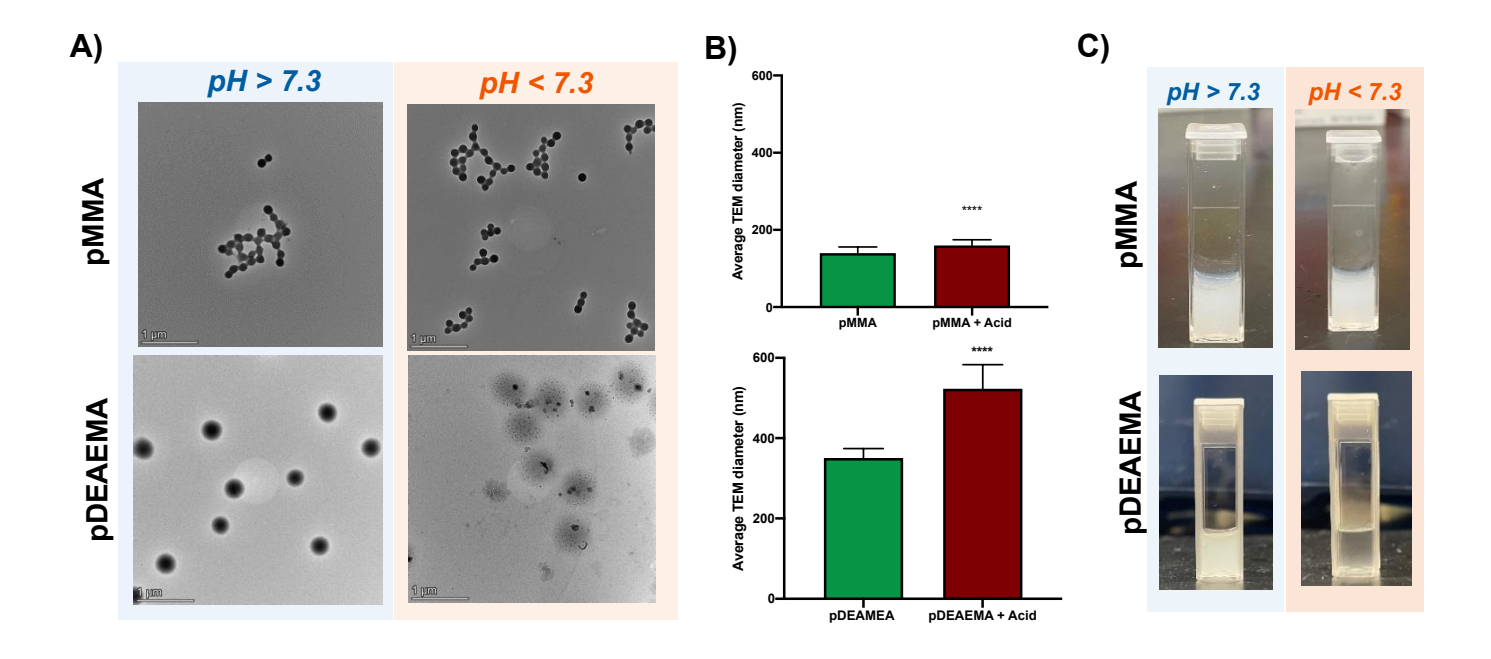


Figure 3: A) Transmission electron micrographs of pMMA and pDEAEMA nanoparticles in basic (pH > 7.3) and acidic (pH < 7.3) media. B) Average TEM diameters of pMMA (top) and pDEAEMA (bottom) nanoparticles in basic (pH > 7.3) and acidic (pH < 7.3) media (N=500, ****p<0.0001). C) Pictures showing turbidity of pMMA and pDEAEMA nanoparticles in basic (pH > 7.3) and acidic (pH < 7.3) media.

Polymer Nanoparticle Size Reversibility

The pH responsiveness of polymer nanoparticles like pDEAEMA has made them an attractive polymer for various applications. $^{7, 39, 40}$ An even more interesting property is that these pH-based transformations are reversible when the original stimuli is removed or changed. 39 This is evident in the data shown in Figure 5 as we cycle through different pH extremes for the same batch of pDEAEMA nanoparticles. At pH 4, the size of pDEAEMA is \sim 670 nm, but decreases back to \sim 380 nm when placed in pH 10. Moreover, the size increases to \sim 640 nm when placed back into acidic media, showcasing the ability to swell, deswell, and reswell for pDEAEMA while pMMA remains constant as a negative control. There is no statistically significant difference in the size of pDEAEMA nanoparticles at the swell state (670 nm) and reswell state (640 nm) which both occur at pH 4 (p = 0.6623). The zeta potential results show that the pH cycling impacts the charge of pDEAEMA as it transitions from being positively charged at pH 4, to negatively charged at pH 10, and back to positively charged at pH 4 while pMMA remains unchanged across the same pH cycle. One of the most exciting opportunities available with reversibly swelling polymeric nanoparticles is the capacity to load small molecule cargo (e.g. to create labeled nanoparticles) and

perhaps deliver that cargo in an alternate pH environment (e.g. drug or nutrient delivery). Herein, we will assess the small molecule loading capacity of the stimuli-responsive polymers using RITC as the proof-of-concept cargo.

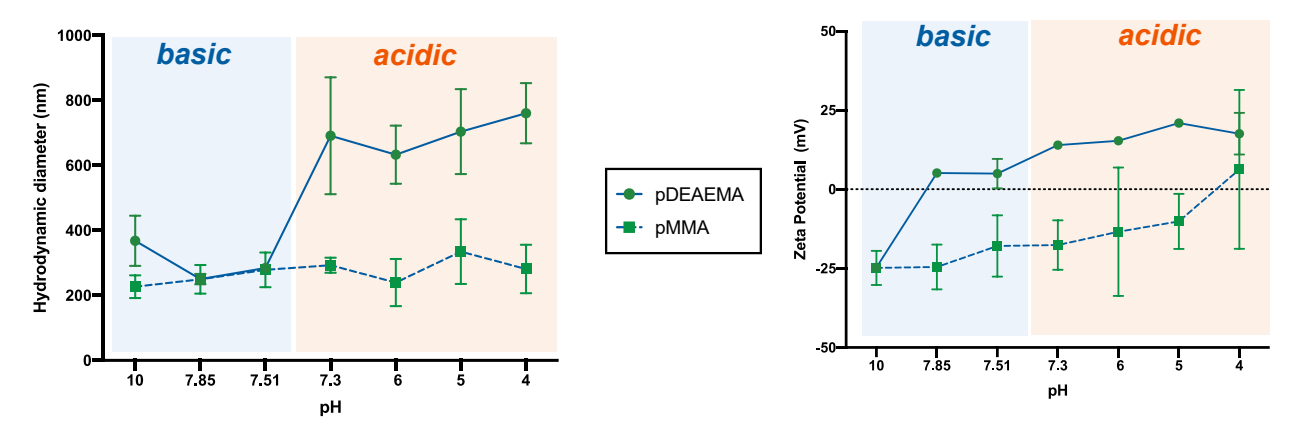


Figure 4: Hydrodynamic diameters and zeta potentials of pDEAEMA (solid line) and pMMA (dashed line) nanoparticles across a range of pHs in potassium phosphate buffers. Error bars represent standard deviation across 3 material replicates.

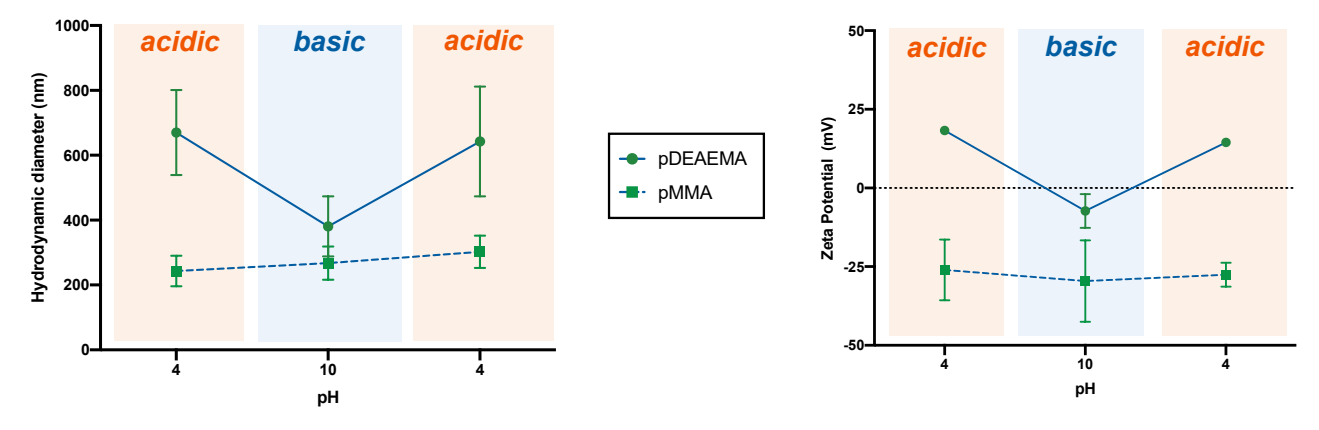


Figure 5: Hydrodynamic diameters and zeta potentials of pDEAEMA (solid line) and pMMA (dashed line) nanoparticles when cycled through pH 4 and pH 10 media. Error bars represent standard deviation across 3 material replicates and are not visible for zeta potential results of pDEAMEA since they are too small.

Polymer Nanoparticle Size Characterization

Ideally, it would be possible to tune the load of cargo taken up into polymeric nanoparticles, and one way to accomplish that is by tuning the size of the nanoparticles. As such, to investigate

the role of pDEAEMA size on the loading and release of RITC, we synthesized polymeric nanoparticles with varied size. With other synthesis all conditions remaining consistent, this work exploited synthesis temperature to obtain size-tunable pDEAEMA nanoparticles, where lower synthesis temperatures resulted in larger hydrodynamic diameters as shown in Figure 6 (here, shown ahead of acid-induced swelling). Since the performance of the radical initiator, ammonium persulfate, is temperature-dependent, the nanoparticle size will be affected by synthesis temperatures.

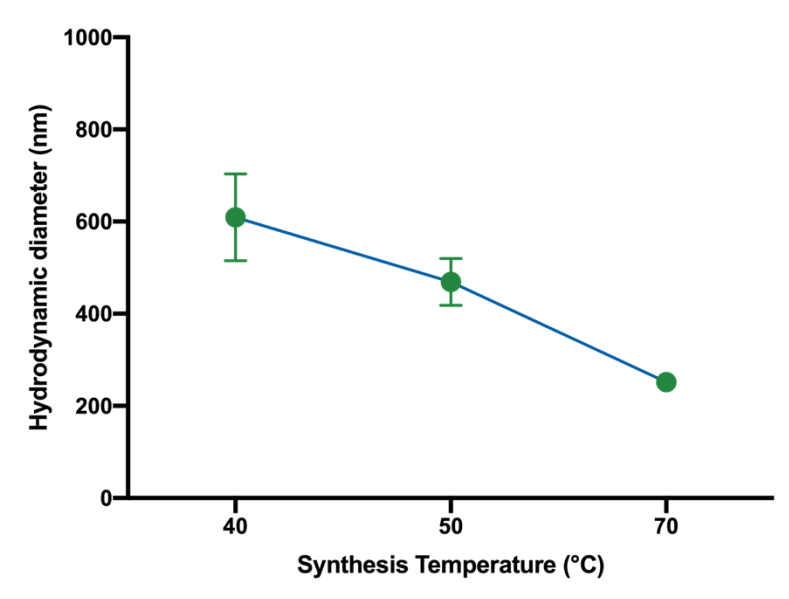


Figure 6: Hydrodynamic diameter of pDEAEMA nanoparticle at pH > 7.3 as a function of synthesis temperature. Error bars represent standard deviation across 3 material replicates and are not visible for 70°C since they are too small.

Higher temperatures increase the radical formation (and polymerization rate) and thus reduce the polymer nanoparticle size while lower temperatures show the opposite effect.⁴¹ Based on this, pDEAEMA nanoparticles with sizes of 610 ± 95 nm, 469 ± 51 nm, and 252 ± 13 nm were prepared at temperatures of 40 °C, 50 °C, and 70 °C, respectively. Further characterization on the swelling of the larger nanoparticles is presented in the Supporting Information.

Dye Loading and Release Characterization

With variable size pDEAEMA polymeric nanoparticles and a control pMMA polymeric nanoparticle, a systematic study of small molecule loading could be undertaken. Figure 7A shows the experimental design used for assessing the loading and release of RITC from pDEAEMA (with diameters of approximately 250 nm, 470 nm, or 600 nm) and 240-nm-diameter pMMA. Briefly, RITC was incubated with the polymer of interest for 1 hour while shaking at 150 rpms in pH 4 media to induce swelling in pDEAEMA. Following this, the solution was added to basic media to allow for dye uptake during polymer shrinking (or deswelling) for the pDEAEMA nanoparticles. After multiple washes to remove any unincorporated dye, the fluorescence of the final nanoparticle suspension was measured in: i) acidic media to promote dye release upon reswelling and ii) basic media, aiming to measure the dye while still contained in the nanoparticle and facilitate comparison. The fluorescence of supernatants of the centrifugates were also saved to assess

progressive decrease in fluorescence after each wash (Figure S6 in Supporting Information). To assess any interferences from the polymer itself, we used a negative control where water replaced RITC as a background subtraction.

Figure 7B shows the fluorescence intensity of these 4 polymeric nanoparticles (the 3 sizes of pDEAEMA and 1 size of pMMA) in PBS or neutral media. For each polymer nanoparticle, we considered a high and low dose of RITC, 19.8 µg/mL and 74.6 µg/mL (denoted as 25 µL and 100 μL), to optimize the amount of dye loaded and evaluate differences in dye loading. As expected, the more dye added, the higher the fluorescence intensity contained within the 3 pDEAEMA nanoparticles presented in Figure 7A. This is likely driven by the hydrophobic nature of pDEAEMA nanoparticles promoting favorable interactions with the hydrophobic RITC molecules.^{25, 42} However, when comparing across different pDEAEMA diameters, there was no statistically significant difference in fluorescence intensity, except when comparing 25 µL of 250 nm and 25 µL of 600 nm. From this, we concluded that nanoparticle size didn't impact the amount of dye loaded as measured by fluorescence intensity, likely suggesting that the dye molecules can only penetrate so far into the nanoparticle structure and even at the smallest size, we have reached a maximum limit. More interestingly, the results of pMMA nanoparticles show a much lower fluorescence than any of the pDEAEMA nanoparticles, and there is also no statistically significant difference when adding 25 µL or 100 µL of RITC, indicating that the fluorescence levels out regardless of a high or low dose of RITC. As the key difference between pDEAEMA and pMMA is the lack of swelling, and thus reversibility of swelling when cycling through different pHs, this result indicates the success of our loading mechanism when comparing pH–sensitive (pDEAEMA) and pH-insensitive (pMMA) polymeric nanoparticles.

An attractive feature of pH-responsive polymers like pDEAEMA is the potential pH-triggered release of loaded cargo when these polymeric nanoparticles are exposed to acidic media. As such, we evaluated the release profile from these loaded pDEAEMA nanoparticles, and since the swelling is immediate, we measured the fluorescence of our nanoparticles right after adding them to pH 4 media. Figure 7C shows the fluorescence of the 3 pDEAEMA nanoparticle diameters (with 250 nm, 400 nm, and 600 nm sizes) and pMMA nanoparticles (240-nm-diameter) in neutral media (deswollen state) or acidic media (swollen state) for the higher dose of added RITC dye (results for low dose RITC are presented in Figure S7 of the Supporting Information). With pMMA nanoparticles, we once again see low fluorescence and no significant difference between neutral

or acidic media. The pDEAEMA nanoparticles show more nuanced results – for all 3 sizes of pDEAEMA nanoparticles, the released dye (in acidic conditions) has a statistically significant decrease in fluorescence than the loaded dye (in neutral conditions). This could be attributed to the dilution of RITC molecules as they are released into solution thereby lowering their fluorescence intensity. When comparing across sizes, there was no statistically significant difference in the acid-treated samples, further indicating that size didn't have a critical impact on the cargo loading and release (though reversibility of the larger nanoparticles still allows for loading to take place where larger particles may be of interest). RITC-loading encapsulation efficiencies for both pMMA and pDEAEMA nanoparticles was calculated based on fluorescence intensities shown in

A) Dye Loading and Release Experimental Design

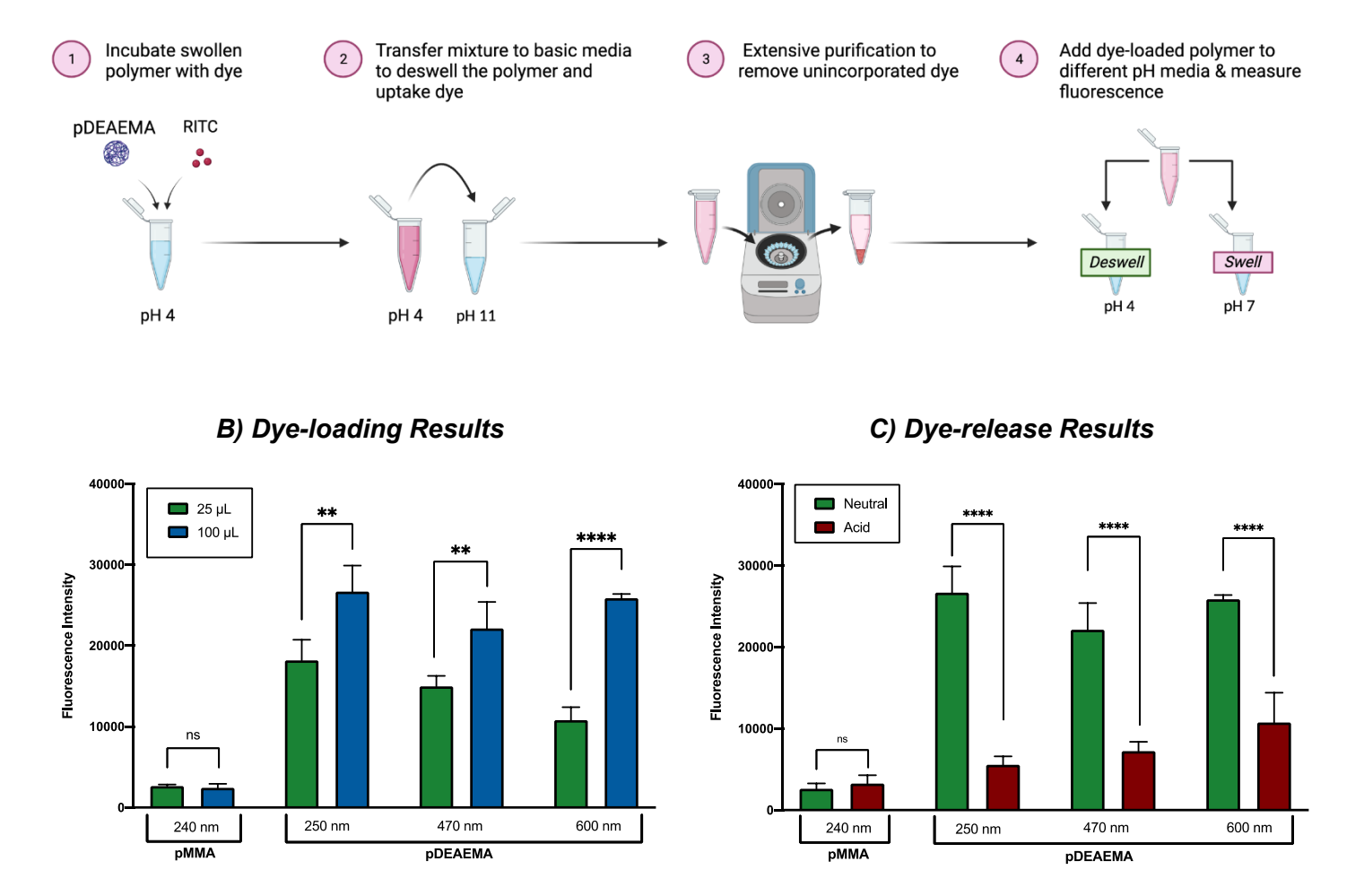


Figure 7: A) Dye loading and release schematic created with <u>BioRender.com</u>, B) Fluorescence intensities of dyeloaded pDEAEMA and pMMA nanoparticles with low and high doses of RITC (250 nm, **p=0.0018, 470 nm, **p=0.0086, 600 nm **** p<0.0001), C) Fluorescence intensities representing dye-release from pDEAEMA and pMMA nanoparticles for high dose RITC (all ****p<0.0001).

Figure 7 (data presented in Supporting Information). As expected, the pDEAEMA nanoparticles had higher encapsulation efficiency (22 – 27 %) compared to pMMA (2.4%). More interestingly, we tested the role of incubation time on the efficiency of our loading strategy (details in Supporting Information). We discovered that our loading strategy allows for dye loading even at a 0-hour incubation which represents the immediate mixing of RITC and the polymer nanoparticle in pH 4 media to swell the polymer followed by the deswelling in pH 11 media to deswell the polymer with no incubation or shaking. This resulted in a 38% RITC loading efficiency proving that our system allows for a rapid and simple loading strategy for pDEAEMA nanoparticles (Figure S9). To better understand nanoparticle behavior, confocal fluorescence microscopy was used to visualize this nanoparticle/RITC fluorescence in swollen and deswollen states.

Confocal Microscopy of RITC-loaded Polymer Nanoparticles

The RITC-loaded pDEAEMA (250-nm-diameter) and pMMA (240-nm-diameter) nanoparticles were imaged in acidic (pH 4.7), neutral (pH 7.4) and basic (pH 10.2) media on an Olympus Fluoview confocal microscope, and representative images with respective regions of interest (ROIs) are shown in Figure 8. For pMMA nanoparticles, some nanoparticles exhibit fluorescence, but with no clear distinction between acidic, neutral, and basic treatments. In contrast, the pDEAEMA nanoparticles in neutral and basic media, show a high contrast image of spherical nanoparticles that exhibit RITC fluorescence. Both the neutral and basic media represent a pH environment greater than 7.3 where the pDEAEMA nanoparticles are in their deswollen state keeping the dye contained within the nanoparticle. The acid-treated pDEAEMA nanoparticles show a lower contrast image, revealing release of the dye from some areas as highlighted by ROIs 1, 2, and 3. As the acidic pH is less than 7.3, the pDEAEMA nanoparticles are in their swollen state where dye release is expected. Image analysis using Fiji also revealed quantitative results that match the qualitative trends seen (shown in Figure S8 in Supporting Information). The mean fluorescence intensity of RITC within the pDEAEMA nanoparticles is higher for the ones in neutral media when compared to acid-treated nanoparticles which parallels data presented in Figure 7. As mentioned above, this could be due to the RITC fluorescence being diluted upon release from the pDEAEMA nanoparticles in acidic media. This can be further visualized by the regions of interest highlighted in Figure 8 (ROI 1, 2, and 3). When comparing the area of the pDEAEMA and pMMA nanoparticles that are fluorescing in Figure 8, only the pDEAEMA nanoparticles exhibited a statistically significant increase in area when placed in acidic media

further indicating that swelling is taking place. It's important to note that the samples size for the pMMA particles was much smaller due to the lack of fluorescent particles present in the image.

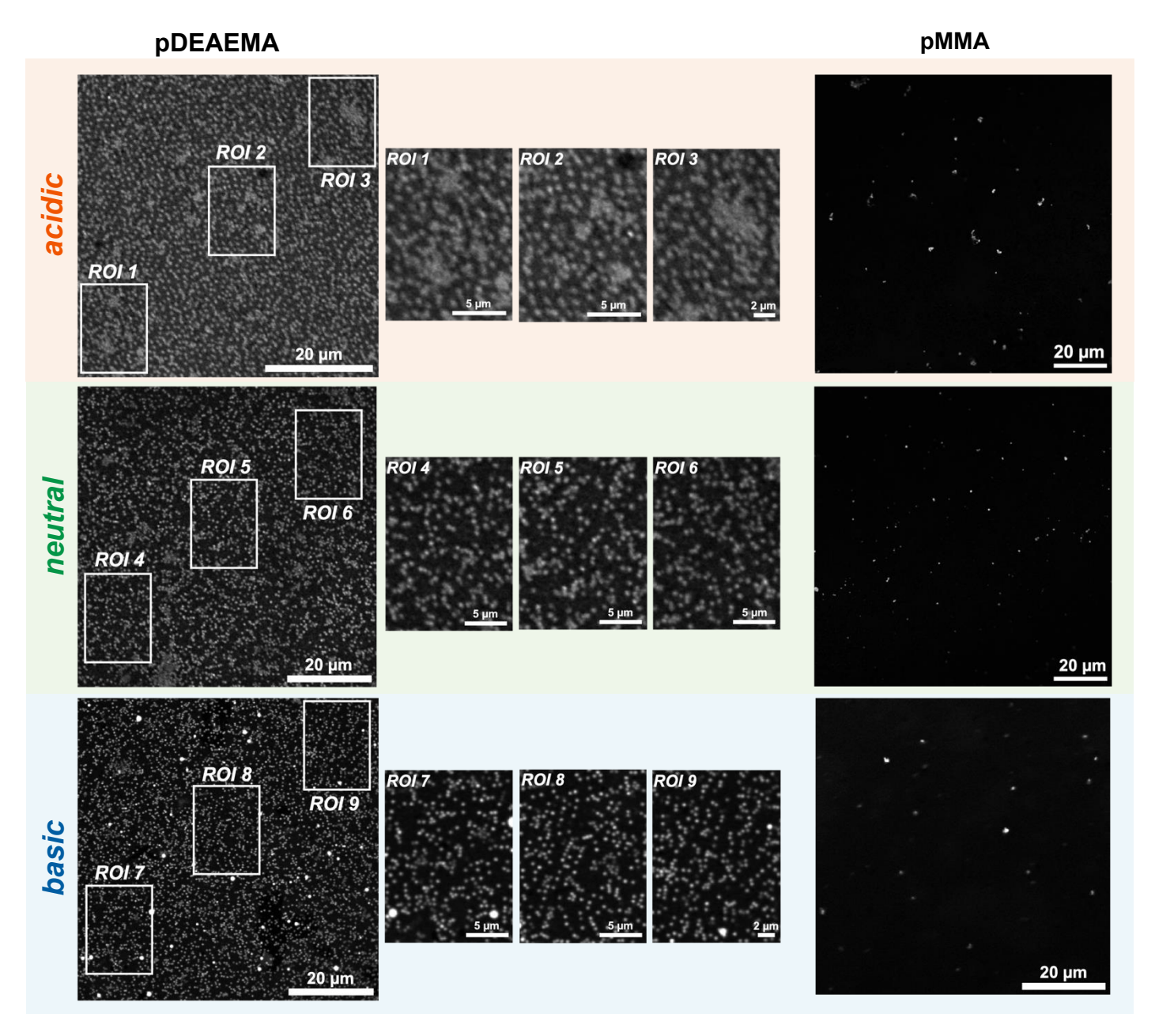


Figure 8: Confocal microscopy images of pDEAEMA (left) and pMMA (right) nanoparticles in acidic (pH 4.7), neutral (pH 7.4) and basic (pH 10.2) media. Insets show regions of interest (ROIs) for pDEAEMA nanoparticles to highlight contrast differences between different pH treatments samples using the QuickFigures plugin in Fiji.

CONCLUSION

The work described herein leveraged the reversible nature of swelling polymeric nanoparticles, when cycled through low, high, and low pH, to load cargo. pDEAEMA nanoparticles were used with a RITC dye as a model cargo to quantify fluorescence differences when nanoparticles are in acidic vs basic media in comparison to the non-swelling control, pMMA. Both nanoparticles show similar characteristics in basic media, but pDEAEMA experiences a size increase when the pH is dropped below 7.3 and this increase can be reversed when the suspension is added to basic media whereas pMMA shows no changes to the nanoparticle size. We also prepared 3 different sizes of pDEAEMA nanoparticles which all showed similar reversible swelling behavior at the 7.3 pH threshold. Our dye loading experiments showcase dye uptake in pDEAEMA nanoparticles due to a notable and significant fluorescence increase when compared to the non-swelling (and thus non-reversible) pMMA nanoparticles. Confocal microscopy images support this result with higher contrast, and numerous, pDEAEMA nanoparticles exhibiting RITC fluorescence whereas pMMA nanoparticles show much lower fluorescence. Upon release in acidic media, pDEAEMA experiences a significant decrease in fluorescence intensity and confocal images show a lower contrast image with specific regions of interest highlighting RITC release while pMMA nanoparticles show no pH-depended differences. We also learned that tuning pDEAEMA size had no impact on loading capacity, but similar trends for pDEAEMA loading were seen across all particles, suggesting that presence of reversibility is the key factor for the success of loading. Lastly, our method allows for dye loading by simply mixing the pDEAEMA nanoparticles with the dye with no time allocated for incubation making this approach a fast and simple loading strategy for pDEAEMA nanoparticles. As this is a proof-of-concept model, future work will focus on using this mechanism to load other beneficial cargo that will facilitate application across a broad range of sectors.

SUPPORTING INFORMATION

The Supporting Information document contains swelling stability at pH 4 and swelling between pH 7.1 - 7.5, SEM images with the experimental details, size, and zeta potential for 470-nm- and 600-nm-diameter nanoparticles, fluorescence intensities of supernatant washes and low dose RITC, image analysis data, RITC encapsulation efficiency, and fluorescence intensity of different incubation times.

ACKNOWLEDGEMNTS

This work was supported by the National Science Foundation under grant no. CHE2001611, the NSF Center for Sustainable Nanotechnology (CSN). The CSN is part of the Centers for Chemical Innovation Program. Parts of this work were carried out in the Characterization Facility, University of Minnesota, which receives partial support from the NSF through the MRSEC (Award Number DMR-2011401) and the NNCI (Award Number ECCS-2025124) programs. This work was supported by the resources and staff at the University of Minnesota University Imaging Centers (UIC). SCR 020997. We want to acknowledge Dr. Michael Odlyzko, University of Minnesota Characterization Facility, Dr. Mary Brown, Dr. Guillermo Marques and Patrick Willey, University of Minnesota University Imaging Centers for their consistent support and guidance. Some figures and schemes were created with BioRender.com. We want to acknowledge Clare Froehlich for SEM images as well as Nick Kreofsky and Punarbasu Roy for help with molecular weight characterization. B.S.T acknowledges support from the University of Minnesota Graduate School's Interdisciplinary Doctoral Fellowship and the Doctoral Dissertation Fellowship. A.T.L acknowledges support from the University of Minnesota Chemistry Department's Heisig/Gleysteen Fellowship and the University of Minnesota Undergraduate Research Opportunities Program (UROP).

References

- 1. Wei, M.; Gao, Y.; Li, X.; Serpe, M. J., Stimuli-responsive polymers and their applications. *Polymer Chemistry* **2017**, *8* (1), 127-143.
- 2. Hu, L.; Zhang, Q.; Li, X.; Serpe, M. J., Stimuli-responsive polymers for sensing and actuation. *Materials Horizons* **2019**, *6* (9), 1774-1793.
- 3. Shu, T.; Hu, L.; Shen, Q.; Jiang, L.; Zhang, Q.; Serpe, M. J., Stimuli-responsive polymer-based systems for diagnostic applications. *Journal of Materials Chemistry B* **2020**, *8* (32), 7042-7061.
- 4. Shao, G.; Liu, Y.; Cao, R.; Han, G.; Yuan, B.; Zhang, W., Thermo-responsive block copolymers: assembly and application. *Polymer Chemistry* **2023**, *14* (16), 1863-1880.
- 5. Hironaka, K.; Yoshihara, E.; Nabil, A.; Lai, J. J.; Kikuchi, A.; Ebara, M., Conjugation of antibody with temperature-responsive polymer via in situ click reaction to enable biomarker enrichment for increased diagnostic sensitivity. *Biomaterials Science* **2021**, *9* (14), 4870-4879.
- 6. Gao, W.; Chan, J. M.; Farokhzad, O. C., pH-Responsive Nanoparticles for Drug Delivery. *Molecular Pharmaceutics* **2010**, *7* (6), 1913-1920.
- 7. Deirram, N.; Zhang, C.; Kermaniyan, S. S.; Johnston, A. P. R.; Such, G. K., pH-Responsive Polymer Nanoparticles for Drug Delivery. *Macromolecular Rapid Communications* **2019**, *40* (10), 1800917.
- 8. Fomina, N.; McFearin, C.; Sermsakdi, M.; Edigin, O.; Almutairi, A., UV and Near-IR Triggered Release from Polymeric Nanoparticles. *Journal of the American Chemical Society* **2010**, *132* (28), 9540-9542.
- 9. Reddy, S. T.; Rehor, A.; Schmoekel, H. G.; Hubbell, J. A.; Swartz, M. A., In vivo targeting of dendritic cells in lymph nodes with poly(propylene sulfide) nanoparticles. *J Control Release* **2006**, *112* (1), 26-34.
- 10. Chauhan, M.; Basu, S. M.; Yadava, S. K.; Sarviya, N.; Giri, J., A facile strategy for the preparation of polypropylene sulfide nanoparticles for hydrophobic and base-sensitive cargo. *Journal of Applied Polymer Science* **2022**, *139* (10), 51767.
- 11. Chauhan, M.; Basu, S. M.; Qasim, M.; Giri, J., Polypropylene sulphide coating on magnetic nanoparticles as a novel platform for excellent biocompatible, stimuli-responsive smart magnetic nanocarriers for cancer therapeutics. *Nanoscale* **2023**, *15* (16), 7384-7402.
- 12. Xu, Q.; He, C.; Xiao, C.; Chen, X., Reactive Oxygen Species (ROS) Responsive Polymers for Biomedical Applications. *Macromolecular Bioscience* **2016**, *16* (5), 635-646.
- 13. Guragain, S.; Bastakoti, B. P.; Malgras, V.; Nakashima, K.; Yamauchi, Y., Multi-Stimuli-Responsive Polymeric Materials. *Chemistry A European Journal* **2015**, *21* (38), 13164-13174.
- 14. Tuga, B.; O'Keefe, T.; Deng, C.; Ligocki, A. T.; White, J. C.; Haynes, C. L., Designing nanoparticles for sustainable agricultural applications. *Trends in Chemistry* **2023**, *5* (11), 814-826.
- 15. Hill, M. R.; Mackrell, E. J.; Forsthoefel, C. P.; Jensen, S. P.; Chen, M.; Moore, G. A.; He, Z. L.; Sumerlin, B. S., Biodegradable and pH-Responsive Nanoparticles Designed for Site-Specific Delivery in Agriculture. *Biomacromolecules* **2015**, *16* (4), 1276-1282.
- 16. Puoci, F.; Iemma, F.; Spizzirri, U. G.; Cirillo, G.; Curcio, M.; Picci, N., Polymer in Agriculture: a Review. *American Journal of Agricultural and Biological Sciences* **2008**, *3* (1), 299-314.
- 17. Xin, X.; He, Z.; Hill, M. R.; Niedz, R. P.; Jiang, X.; Sumerlin, B. S., Efficiency of Biodegradable and pH-Responsive Polysuccinimide Nanoparticles (PSI-NPs) as Smart

- Nanodelivery Systems in Grapefruit: In Vitro Cellular Investigation. *Macromol Biosci* **2018**, *18* (7), e1800159.
- 18. Such, G. K.; Yan, Y.; Johnston, A. P. R.; Gunawan, S. T.; Caruso, F., Interfacing Materials Science and Biology for Drug Carrier Design. *Advanced Materials* **2015**, *27* (14), 2278-2297.
- 19. Sattelmacher, B., The apoplast and its significance for plant mineral nutrition. *New Phytologist* **2001**, *149* (2), 167-192.
- 20. Geilfus, C.-M., The pH of the Apoplast: Dynamic Factor with Functional Impact Under Stress. *Molecular Plant* **2017**, *10* (11), 1371-1386.
- 21. Kocak, G.; Tuncer, C.; Bütün, V., pH-Responsive polymers. *Polymer Chemistry* **2017**, *8* (1), 144-176.
- 22. Elsabahy, M.; Wooley, K. L., Design of polymeric nanoparticles for biomedical delivery applications. *Chemical Society Reviews* **2012**, *41* (7), 2545.
- 23. Cayre, O. J.; Chagneux, N.; Biggs, S., Stimulus responsive core-shell nanoparticles: synthesis and applications of polymer based aqueous systems. *Soft Matter* **2011**, *7* (6), 2211-2234.
- 24. Liu, H.; Lin, S.; Feng, Y.; Theato, P., CO2-Responsive polymer materials. *Polymer Chemistry* **2017**, *8* (1), 12-23.
- 25. Hu, Y.; Litwin, T.; Nagaraja, A. R.; Kwong, B.; Katz, J.; Watson, N.; Irvine, D. J., Cytosolic Delivery of Membrane-Impermeable Molecules in Dendritic Cells Using pH-Responsive Core—Shell Nanoparticles. *Nano Letters* **2007**, *7* (10), 3056-3064.
- 26. Yang, Z.; Chen, H., The recent progress of inorganic-based intelligent responsive nanoplatform for tumor theranostics. *VIEW* **2022**, *3* (6), 20220009.
- 27. Wong, A. S. M.; Mann, S. K.; Czuba, E.; Sahut, A.; Liu, H.; Suekama, T. C.; Bickerton, T.; Johnston, A. P. R.; Such, G. K., Self-assembling dual component nanoparticles with endosomal escape capability. *Soft Matter* **2015**, *11* (15), 2993-3002.
- 28. Kern, H. B.; Srinivasan, S.; Convertine, A. J.; Hockenbery, D.; Press, O. W.; Stayton, P. S., Enzyme-Cleavable Polymeric Micelles for the Intracellular Delivery of Proapoptotic Peptides. *Molecular Pharmaceutics* **2017**, *14* (5), 1450-1459.
- 29. Sun, J.-T.; Hong, C.-Y.; Pan, C.-Y., Fabrication of PDEAEMA-Coated Mesoporous Silica Nanoparticles and pH-Responsive Controlled Release. *The Journal of Physical Chemistry C* **2010**, *114* (29), 12481-12486.
- 30. Zhang, F.; Niu, Y.; Li, Y.; Yao, Q.; Chen, X.; Zhou, H.; Zhou, M.; Xiao, J., Fabrication and characterization of structurally stable pH-responsive polymeric vesicles by polymerization-induced self-assembly. *RSC Advances* **2021**, *11* (46), 29042-29051.
- 31. Yang, C.; Xiao, J.; Xiao, W.; Lin, W.; Chen, J.; Chen, Q.; Zhang, L.; Zhang, C.; Guo, J., Fabrication of PDEAEMA-based pH-responsive mixed micelles for application in controlled doxorubicin release. *RSC Advances* **2017**, *7* (44), 27564-27573.
- 32. Chen, Q.; Lin, W.; Wang, H.; Wang, J.; Zhang, L., PDEAEMA-based pH-sensitive amphiphilic pentablock copolymers for controlled anticancer drug delivery. *RSC Advances* **2016**, *6* (72), 68018-68027.
- 33. Zhang, L.; Zhang, C.; Gu, X.; Wang, G., Self-assembly, pH-responsibility and controlled release of doxorubicin of PDEAEMA-PEG-PDEAEMA triblock copolymers: effects of PEG length. *Journal of Polymer Research* **2021**, *28* (5), 175.
- 34. Yang, C.; Wang, D.; Liu, W.; Yang, Z.; He, T.; Chen, F.; Lin, W., Folate modified dual pH/reduction-responsive mixed micelles assembled using FA-PEG-PDEAEMA and PEG-SS-PCL for doxorubicin delivery. *Physical Chemistry Chemical Physics* **2023**, *25* (17), 12458-12468.

- 35. Liu, W.; Li, J.; Qin, Z.; Yao, M.; Tian, X.; Zhang, Z.; Zhang, L.; Guo, Q.; Zhang, L.; Zhu, D.; Yao, F., Zwitterionic Unimolecular Micelles with pH and Temperature Response: Enhanced In Vivo Circulation Stability and Tumor Therapeutic Efficiency. *Langmuir* **2020**, *36* (13), 3356-3366. 36. Zhang, Y.; Ang, C. Y.; Li, M.; Tan, S. Y.; Qu, Q.; Luo, Z.; Zhao, Y., Polymer-Coated Hollow Mesoporous Silica Nanoparticles for Triple-Responsive Drug Delivery. *ACS Applied Materials & Interfaces* **2015**, *7* (32), 18179-18187.
- 37. Wang, N.; Cheng, X.; Li, N.; Wang, H.; Chen, H., Nanocarriers and Their Loading Strategies. *Advanced Healthcare Materials* **2019**, *8* (6), 1801002.
- 38. Vrignaud, S.; Benoit, J.-P.; Saulnier, P., Strategies for the nanoencapsulation of hydrophilic molecules in polymer-based nanoparticles. *Biomaterials* **2011**, *32* (33), 8593-8604.
- 39. Park, I. K.; Singha, K.; Arote, R. B.; Choi, Y. J.; Kim, W. J.; Cho, C. S., pH-Responsive Polymers as Gene Carriers. *Macromol Rapid Commun* **2010**, *31* (13), 1122-33.
- 40. Xie, J.; Li, A.; Li, J., Advances in pH-Sensitive Polymers for Smart Insulin Delivery. *Macromolecular Rapid Communications* **2017**, *38* (23), 1700413.
- 41. Tunc, Y.; Ulubayram, K., Production of highly crosslinked microspheres by the precipitation polymerization of 2-(diethylamino)ethyl methacrylate with two or three functional crosslinkers. *Journal of Applied Polymer Science* **2009**, *112* (1), 532-540.
- 42. Cingolani, M.; Rampazzo, E.; Zaccheroni, N.; Genovese, D.; Prodi, L., Fluorogenic hyaluronan nanogels for detection of micro- and nanoplastics in water. *Environmental Science: Nano* **2022**, *9* (2), 582-588.